

Notes

The X21 SAXS Instrument at NSLS for Studying Macromolecular Systems

Lin Yang*

National Synchrotron Light Source, Brookhaven National Laboratory, Upton, NY 11973, USA

Received , 2005; Revised , 2005

Introduction

The beamline X21 at NSLS was originally designed for Inelastic X-ray Scattering (IXS) because of its high-flux 27-pole wiggler source. The downstream and upstream endstations at the beamline had been respectively occupied by the original phase I and its succeeding phase II of the IXS instrument.^{1,2} In 2003, in recognition of the rising demand for high-flux elastic scattering, particularly SAXS, NSLS rebuilt the beamline and shifted its research focus. The high energy-resolution 4-bounce monochromator used for phase II IXS² was replaced with a monochromator with interchangeable Si(111) and ML elements.³ The two sets of crystals sit side-by-side on the same spindle and with their first crystals that reflect the white beam cryogenically cooled by a cold helium gas refrigerator to near 70 K, where the thermal conductivity of silicon is high and its thermal expansion coefficient is low, therefore improving beam stability against heat load variation on the monochromator. A new toroidal mirror was also installed to deliver monochromatic beam into the downstream endstation. The two endstations now operate in series in a mutually exclusive fashion. The upstream endstation now hosts a high magnetic field scattering program. The downstream endstation is chosen for SAXS because of its large size (~5 m in the direction of the beam) and long distance from the source. This note describes the design of some key components of the X21 SAXS instrument and the representative results obtained during its commissioning in the summer of 2004.

Instrumentation

The overall layout of the SAXS instrument at X21 is shown in Figure 1. The x-ray energy is selected by the Si/ML monochromator described above. For the measure-

ments in which the energy resolution is important (e.g. anomalous scattering), the Si(111) crystals are used. On the other hand, when higher x-ray flux is desirable, the ML elements can be used to give a > 50x increase in beam intensity at the expense of broader energy resolution (~1%). When the Si crystals are used, the x-ray energy range is limited by the reflectivity of the toroidal mirror to ~20 KeV. For ML elements, the energy range is limited to up to ~11 keV because the first multilayer would not be able to capture the full beam coming from the wiggler at shallow incident angles due to the relatively large beam size in the vertical direction. The measured x-ray flux is shown in Figure 2.

Located at 19 m from the source is the toroidal mirror, bendable in the meridional direction so that the monochromatic beam can be focused at different locations. Although ideally the x-ray beam can be focused into a 0.9×0.4 mm spot (FWHM, by simulation, assuming beam focused at the sample), in order to minimize the background scattering from in the instrument itself,⁴ the actual beam size and divergence are defined by three sets of high-precision, vacuum-compatible slits (Advanced Design Consulting, Lansing, NY) and the x-ray beam is focused at the midpoint between S_1 and S_2 to allow maximum photon flux at the sample. The slits all have polished tantalum blades and are located at 4, 1 and 0.1 m upstream of the sample. The first two sets of slits are normally set at 0.4×0.4 mm, resulting in ~1.7% (measured) of the full beam flux at the sample. The photon flux can be adjusted by the attenuator located just upstream of S_1 and monitored after S_2 by a *Bicron* scintillation detector that measures the scattering from a retractable thin Mylar film reflector (Figure 1, I).

All beam paths are under vacuum maintained at $< 10^{-2}$ mbar by an oil-free Tri-Scroll pump. The scattering flight tube consists of commercially available 8" stainless steel fittings with LF flanges. Combinations of fittings give sample-to-detector distances from 0.4 m to ~3 m. The cup-shaped beamstop at the end of the beam path is ~3 mm in diameter and also serves as a transmitted beam monitor. Unlike some of the reported photodiode beam monitor embedded into the beamstop, this beamstop is made of solid metal (both brass and tantalum have been used) and rely on the photocurrent produced by blocked x-ray beam to indicate beam intensity. This beam monitor has been calibrated against the *Bicron*-based monitor upstream and found to have good linearity (Figure 3). However, since the photocurrent is often less than 1 nA, this monitor works best when the beam intensity is high and the photocurrent can be accurately measured. The beamstop photocurrent provides a sufficient means of relatively normalizing the data for the purpose for background subtraction. This beam monitor is

*Corresponding Author. E-mail: lyang@bnl.gov

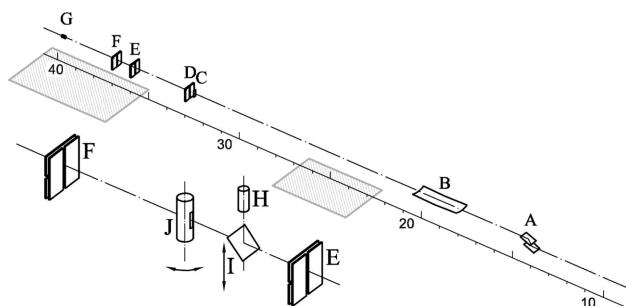


Figure 1. The overall layout of the SAXS instrument at X21. The numbers are the distance (meters) from the source. A: monochromator. B: mirror. C: attenuator. D: S_1 . E: S_2 . F: S_3 . G: beam stop. H+I: beam monitor. J: shutter. The shaded areas represent the experimental stations.

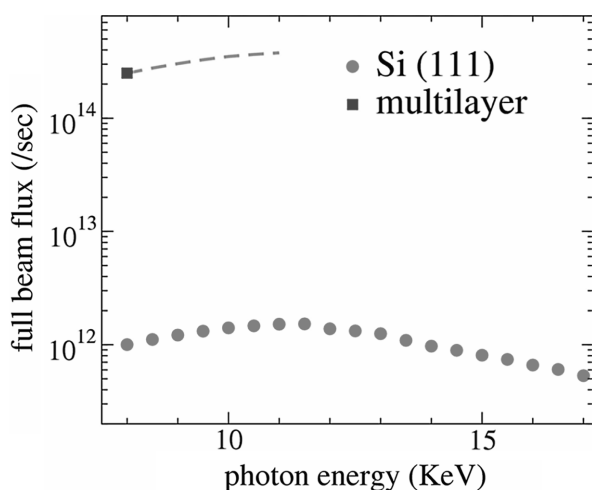


Figure 2. Full beam monochromatic x-ray flux using the Si(111) (red) and the ML (blue) elements of the monochromator. Measured using an ionization chamber. Only one data point was measured for ML. The dashed line is rescaled from Si(111) curve. The energy range when the ML is used is limited to ~ 11 KeV due to geometrical constraints.

also useful for aligning the sample. For instance, in protein solution scattering measurements, it is important that the center of cylindrical capillary tube coincides with beam center so that there will not be any reflection of parasitic slit scattering from the capillary tube. A scan of capillary tube position using this monitor as the detector can be performed. The position with most absorption for a filled tube, or the center between the two absorption peaks that correspond to the capillary walls of an empty tube, is the correct sample position.

The Linux-based beamline control computer runs *fourc* (Certified Scientific Software, Cambridge, MA) on top of *EPICS* to control all motors and detectors on the beamline, including the 13 cm MarCCD detector under the remote control mode. Other instruments, such as temperature con-

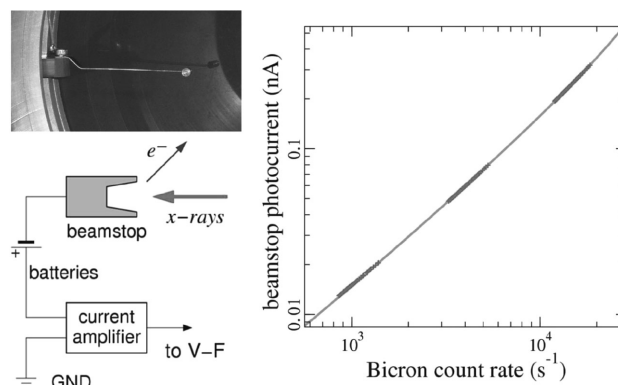


Figure 3. The schematic (lower left) of the solid metal beamstop (upper left) used as a beam monitor and its calibration against the *Bicron* monitor (Fig1.H) (right). The amplified photocurrent is converted into pulses by a V-F converter and fed to a counter. The red symbols in the calibration curve is the data and the continuous line is the fit, assuming linear response from the beamstop and that the *Bicron* detector has a deadtime of $9.9 \mu\text{s}$.

troller, syringe pump and water circulator, are also controlled from *fourc* through serial ports. The scripting (macros) capability of *fourc* allows for automated data collection by the CCD detector in concert with the sample changer and/or the temperature controller. Simple remote data collection is also possible using utility program available in Linux (e.g. remote display, and *connect*⁵).

A GUI data processing program is available on the beamline control computer for simple data processing. Besides displaying data with customizable color scale and magnification, this program also provides the capability of flat field correction, extracting line profiles from the data, subtraction of background and performing angular integral with masks that block off unwanted regions on the detector (e.g. dead pixels, pixels behind the beamstop). For multiple datasets collected using the same scattering geometry, this program can also process specified datasets on one click.

Scientific Results

The X21 SAXS instrument has hosted a number of user experiments since it was commissioned in the summer of 2004. Existing user programs include protein solutions scattering, grazing incidence small and wide angle scattering from lipid and polymer thin films, and SAXS from biological tissues in water, among others.

Protein solution scattering. This instrument is optimized for measurements that require low scattering background: all beam paths are maintained under vacuum at $< 10^{-2}$ mbar and the slit positions are well separated to ensure a tight beam spot. For solution scattering, a specially designed sample cell consisting of a 1mm glass capillary tube sealed by O-rings across the vacuum beam path (see Figure 4A),

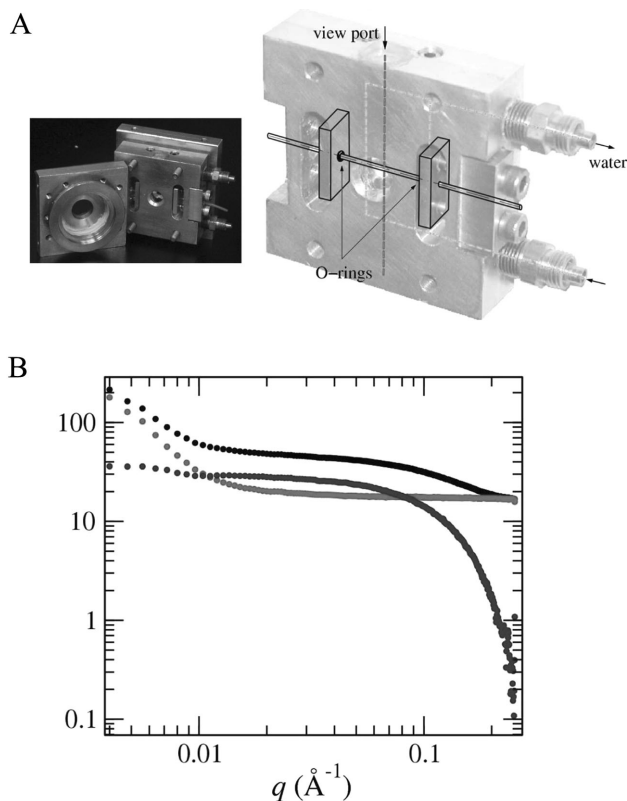


Figure 4. (A) The sample cell used for protein solution scattering. The cell is clamped between two flanged coupling pieces that connect to the rest of vacuum beam path. The capillary tube is held by two O-rings that form the vacuum seal. The cell also features embedded water channels for temperature control and viewports that allow visual monitoring of the sample. (B) A typical solution scattering curve (black) from 5 mg/ml cytochrome-C in 10 mM K_3PO_4 (pH=8.4), as compared to the scattering from buffer solution alone (red). The background-subtracted protein scattering is shown in blue. The exposure time was 30s.

eliminating any extra windows in the beam path that might produce more background scattering. The capillary holder is made of aluminum with embedded water channels and fittings for chilled water to keep the sample at desired temperature. In order to avoid radiation damage, the sample is usually flown through the capillary during x-ray exposure by a syringe pump, which is activated by the beamline control computer just before it opens the x-ray shutter, and the flow can be visually monitored through Plexiglas windows using a video camera.

A typical protein solution scattering curve from cytochrome-C solution, as compared to scattering from the buffer solution, is shown in Figure 4B. Since the scattering intensity from each molecule is proportional to the square of the total electron number, for large molecules, usable scattering data can be collected from solutions of at a concentration as low as 5 μM (SARS main protease, 34 KDa, mixture

of dimers and monomers, 0.17 mg/ml).⁶

With ML monochromator, each protein solution scattering measurement usually completes in ~30 seconds. Short measurement time makes the time needed for changing the samples a significant overhead. An effort is currently under way to realize high throughput solution scattering using a commercial liquid handler. In each cycle of high throughput operation, the liquid handler feeds the solution sample from standard multi-well microplates into the capillary cell and flows the sample through upon receiving the signal from the beamline control computer when the x-ray shutter opens. Once the shutter closes after the measurement completes, the liquid handler flushes the capillary tube with buffer solution and gets ready for next sample.

Grazing incidence scattering. Grazing Incidence scattering at both wide and small angles can be performed at X21. At the longest sample-to-detector distance of ~3 m, the entire detector covers up to $\sim 0.15 \text{ \AA}^{-1}$ in reciprocal space; whereas the maximum q can reach $\sim 2 \text{ \AA}^{-1}$ with a very short scattering beam path. Such grazing incidence geometry is ideal for studying the structures in organic thin films such as polymer nanostructures, organic semiconductors,⁷ and aligned lipid films.⁸ The examples of SAXS and WAXS patterns using grazing incidence geometry are shown in Figure 5.

Clearly, the q -resolution in the WAXS pattern is far from ideal (peak width nearly 0.1 \AA^{-1} for the peak with highest scattering angle). This is because in grazing incidence scattering measurements using an area detector, the q -resolution deteriorates at wide scattering angles due to the parallax effect induced by the finite beam footprint, l , on the sample: $l = a/\sin\alpha$, where a is the vertical beam size and α is the incident angle. As the scattering angle increases, the pixels accept diffraction from a nominally larger sample ($\sim l\sin 2\theta$). This problem can be alleviated with a smaller vertical beam size. A secondary vertical focusing mirror was recently installed for this purpose. Preliminary results show that the focused beam height is less than 8 μm , which translates to a

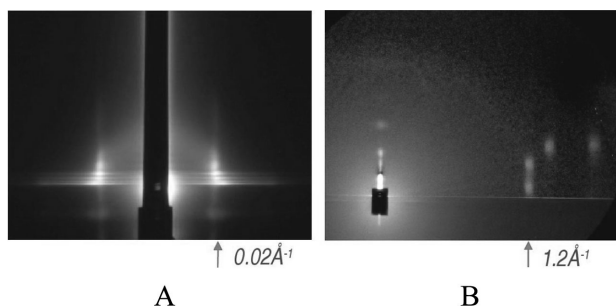


Figure 5. Grazing incidence scattering patterns from (A) a Styrene-Isoprene-Styrene tri-block copolymer hexagonal structure and (B) a thin film of organic semiconductor fluorene-bithiophene-fluorene.⁷

footprint of < 1 mm on the sample assuming an incident angle of 0.5° . With 8 keV x-rays, sample-to-detector distance $d=30$ cm and scattering angle $2\theta=20^\circ$ ($q=1.4 \text{ \AA}^{-1}$), $l=1$ mm translates to $\delta(2\theta)=l\sin 2\theta/\cos 2\theta d=1.1$ mrad and a q -resolution of 0.005 \AA^{-1} , which is sufficient for most measurements on organic thin films.

Thick samples. The x-ray transmission and scattering intensity decrease as the sample thickness increases (for instance, the transmission of 8 keV photons through 1 mm water is 36%, compared to 0.6% at 5 mm). The ability of this instrument to work at higher x-ray energies not only enables anomalous SAXS at a wide range of absorption edges, but also makes experiments with thick samples or samples with high electron density possible. Again using water as an example, the x-ray transmission for 5 mm water increases to 15% at 11 keV and 53% at 16 keV. This benefit is clearly demonstrated in experiments on connective tissue samples (1 mm thick) kept in water (5 mm thick), where the diffraction pattern from collagen fibers was obtained in a few seconds using the ML monochromator at 11 KeV, whereas 20 mins are required at 8 KeV with Si(111) monochromator.⁹

Conclusions

The SAXS instrument at X21 was commissioned in the summer of 2004 and had been accepting general users since. The theme of the scientific programs on this instrument is structural characterization of soft condensed matter and bio-

materials, as represented by the experiments described in this note. General user proposals for beam time on this instrument are accepted through both NSLS and the Center of Functional Nanomaterials (CFN). The NSLS is planning to replace X21 SAXS with an undulator-based instrument. The new instrument, to be located at beamline X9, is currently been designed and scheduled to go on-line by the end of 2007.

References

- (1) C.-C. Kao, K. Hamalainen, M. Krisch, D. P. Siddons, T. Oversluizen, and J. B. Hastings, *Rev. Sci. Instr.*, **66**, 1699-1702 (1995).
- (2) W. A. Caliebe, C.-C. Kao, M. Krisch, T. Oversluizen, P. Montanez, and J. B. Hastings, *AIP Conference Proc.*, **417**, 6-9 (1997).
- (3) L. E. Berman, W. A. Caliebe, P. A. Montanez, L. Yang, C. S. Nelson, A. Lenhard, F. A. Staicu, C. Stelmach, S. C. LaMarr, S. Pjerov, and S. L. Hulbert, to be published.
- (4) B. Chu and B. Hsiao, *Chem. Rev.*, **101**, 1727-1761 (2001).
- (5) <http://www.certif.com/goodies/kibitz/doc.html>. *connect* is based on *expect*, see <http://expect.nist.gov/>.
- (6) V. Graziano, L. Yang, W. McGrath, and W. Mangel, manuscript in preparation.
- (7) T. Shin, H. Yang, L. Yang, B. Lee, M.-M. Ling, M. Roberts, and Z. Bao, unpublished.
- (8) L. Yang and M. Fukuto, *Phys. Rev. E.*, **72**, 010901 (2005).
- (9) J. Liao, L. Yang, J. Grashow, and M. S. Sacks, *Acta Biometeorologia*, **1**, 45-54, 2005.